A Review on Fabrication Technologies for the Monolithic Integration of Tapers with III–V Semiconductor Devices

Ingrid Moerman, *Member, IEEE,* Peter P. Van Daele, *Member, IEEE,* and Piet M. Demeester, *Member, IEEE*

(Invited Paper)

Abstract—The past few years a lot of effort has been put in the development and fabrication of III–V semiconductor waveguiding devices with monolithic integrated mode size converters (tapers). By integrating a taper with a waveguide device, the coupling losses and the packaging cost of OEIC's in future fiber-optical networks can be much reduced. This paper gives an overview of different taper designs, the possible fabrication technologies and performances of tapered devices.

Index Terms— Mode-size converters, monolithic integration, optoelectronic integrated circuits, III–V semiconductors.

I. INTRODUCTION

OPTICAL communication systems are expected to play an increasing role in the transmission and processing of the huge amounts of data. Due to the very large bandwidth of an optical glass fiber, in particular when several optical signals share the same fiber [wavelength division multiplexing or (WDM)], very high transmission capacities can be obtained. Not only in long-haul fiber transmission systems, but also in highly advanced computer networks and electronic systems, there is a need for optical links, as optical interconnections allow to increase the bandwidth and the integration density compared to electrical interconnections.

Most of the building blocks of an fiber-optical network consist of III–V semiconductor devices. As each of these devices is connected to at least one optical fiber, it is of major importance to obtain an efficient coupling of light between fiber and optoelectronic device. The very small refractive index difference in a glass fiber ($\Delta n < 5 \times 10^{-3}$) results in a weakly guided optical mode with a typical mode size of 8–10 μm. In semiconductor waveguiding devices, such small refractive index differences can only be achieved with extremely small compositional changes. In an optimized semiconductor waveguide component, however, Δn is generally larger than 1×10^{-2}, leading to mode sizes smaller than 2 μm. Besides, unlike the circular mode in a fiber, the mode shape in a semiconductor device is highly asymmetric, resulting in an additional mode mismatch between the fiber mode and the semiconductor waveguide mode. It is obvious that the coupling loss between

an optoelectronic device and a fiber is a significant part of the power budget in an optical network.

There are several approaches to improve the fiber-chip coupling efficiency, such as the use of microlenses or tapered/lensed fibers [1], [2]. However, those approaches still suffer from the field mismatch problem, since only the size and not the shape of the optical mode is converted. The reduction of the coupling loss is usually at the expense of the alignment tolerance, resulting in very high packaging costs. Packaging costs can be as high as 90% of the total device cost. Another approach to reduce fiber-chip coupling losses, is the insertion of a silica-based waveguiding module containing a mode-field converting waveguide, in between the fiber and the III–V semiconductor chip [3]–[5]. The silica-based technology allows refractive index differences between core and cladding up to 1×10^{-2}, enabling small modefield sizes which can be matched to III–V semiconductor waveguides. Although good mode-matching and high-coupling efficiencies can be obtained, the small alignment tolerances at the III–V semiconductor interface still hinder easy and low-cost packaging.

During the past years, many researchers have therefore focused on the monolithic integration of mode size converters with III–V semiconductor components, in order to achieve a larger and more symmetric near field pattern at the device facet. The latter approach allows both low coupling loss and large alignment tolerances, and, hence, reduced packaging costs.

In the specific case of the integration of spot-size converters with semiconductor lasers, there is even a twofold advantage: next to the improvement of the coupling efficiency, there is also an increase of the operating lifetime and the maximum output power [6]. Generally, the layer structure of a low threshold laser is optimized toward maximal overlap between optical mode and active layers, resulting in a wide vertical beam divergence [Fig. 1(a)]. In order to reduce the vertical beam divergence, one can decrease the active layer thickness, but this results in a high threshold current [Fig. 1(b)]. When a spot-size converter is integrated with the laser, the optical mode will spread due to the thinner active layer near the laser mirror, and a narrow beam is emitted [Fig. 1(c)]. In this way, the low threshold current, which is determined by the thicker active
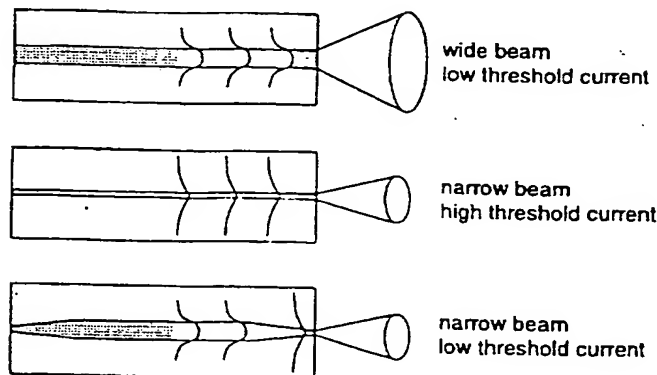
Fig. 1. Optimization of the beam divergence of a laser diode by reduction of the active layer thickness.

layer in the inner region, can be maintained. Furthermore, the large mode-size near the laser mirror enables the reduction of the optical power density, so that the COD (catastrophic optical damage) power level becomes higher, which means that the maximum output power and the operating life increases. It should, however, be noted that for low cost lasers, where a very low threshold current is not an issue, there is a trend to not integrate a spot-size converter, but rather modify the vertical laser structure in order to obtain a large vertical optical mode-size, e.g., by using low refractive index active layers [7], by using diluted waveguide confinement layers [8], by adding extra-thin high-index guide layers in the cladding layers [9] or by using thin wide-gap barriers [10]. Laser diodes without integrated spot-size converter will not be further considered within this paper.

This paper gives an overview of the different technological approaches for the monolithic integration of mode size converters (or tapers) with III–V semiconductor devices, in particular waveguides and laser diodes. Section II gives an overview of the possible taper designs reported by different researchers. In Section III, the different technologies to fabricate tapered devices are reviewed. Finally, an overview is given of the performances achieved for tapered waveguides, in Section IV, and for tapered laser diodes, in Section V.

Before moving to Section II, we want to remark, that a similar review paper has been written a good three years ago [11]. As during the past three years, the number of activities and publications on tapered devices has increased exponentially, this review paper includes the progress that has been made during the past three years and is therefore much more complete.

II. TAPER DESIGNS

A. Introduction

During the past years, many taper designs have been reported. In this section, we have tried to catalogue the major taper designs. For the discussion of the different designs, we make a classification between lateral, vertical, combined and special tapers designs. We limit ourselves in this section by describing different taper layouts, it is not our intention to dis-

cuss taper design rules or to define optimal taper dimensions. For more information on taper design criteria, we refer to [11] and references therein.

Prior to discussing the different taper designs, we would like to comment on the optimal optical mode shape at the tapered end facet of the III–V semiconductor device. The lowest coupling losses (or field mismatch losses) are achieved when the semiconductor waveguide optical mode and the fiber-optical mode are fully matched. The optical mode in a fiber has a quasi-Gaussian shape. Therefore, tapered waveguides are often designed to have a Gaussian mode-profile at the waveguide output facet. A large Gaussian field distribution can only be obtained with a very thick guiding layer which has a very small refractive index difference (order 10^{-3}) with respect to the cladding layers. As already stated in the introduction, such a small refractive index difference can hardly be realized by compositional changes. A more realistic solution is based on the use of homostructure waveguides [12] or diluted structures [13], [14]. The former structures consist of a nonintentionally doped layer (low n-type background concentration) deposited on a highly doped n-type substrate, which has a slightly lower refractive index. In the latter structures, alternated layers of e.g., InGaAsP or InAlAs and InP produce the required equivalent index of the waveguide core. Generally it is difficult to integrate these fiber-matched waveguide structures with other devices. Therefore, Kasaya *et al.*, has demonstrated that very low-loss butt-coupling is also achievable between the Gaussian-shaped fiber mode and the non-Gaussian (exponential-) shaped mode of a semiconductor waveguide with a very thin core [15]. He calculated that InGaAsP–InP waveguide structures can be connected to single-mode fibers with coupling losses below 0.5 dB.

B. Lateral Tapers

In a laterally tapered device, the width of the guiding layer(s) is changed. Possible ways for realizing lateral tapers are presented in Fig. 2. All tapers in this and next figures have, for the ease of drawing, a linear profile. The dark parts in the different tapered waveguide structures represent guiding layers. All tapers are such drawn that the back facet has a small mode-size, whereas the front facet has a large mode-size. The most simple and straightforward designs are those where only the width of the waveguide is changed without affecting the vertical waveguide structure, such as illustrated in Fig. 2(a) for a laterally down-tapered buried waveguide [16] and in Fig. 2(b) for a laterally up-tapered buried waveguide [17]. A simple lateral taper is often applied for high-power laser diodes or semiconductor amplifiers [18]. As the optical beam propagates from the small end of the taper to the large end, it expands laterally, owing to diffraction, thereby spreading the optical power over a wider region. Because of the lateral taper, output powers about an order of magnitude higher than conventional narrow-striped lasers can be obtained.

A lot of mode size converters consist of overlapping waveguides, which means that one waveguide is part of, or surrounded by, a second waveguide. The optical power is coupled from one waveguide to the other by means of a tapered
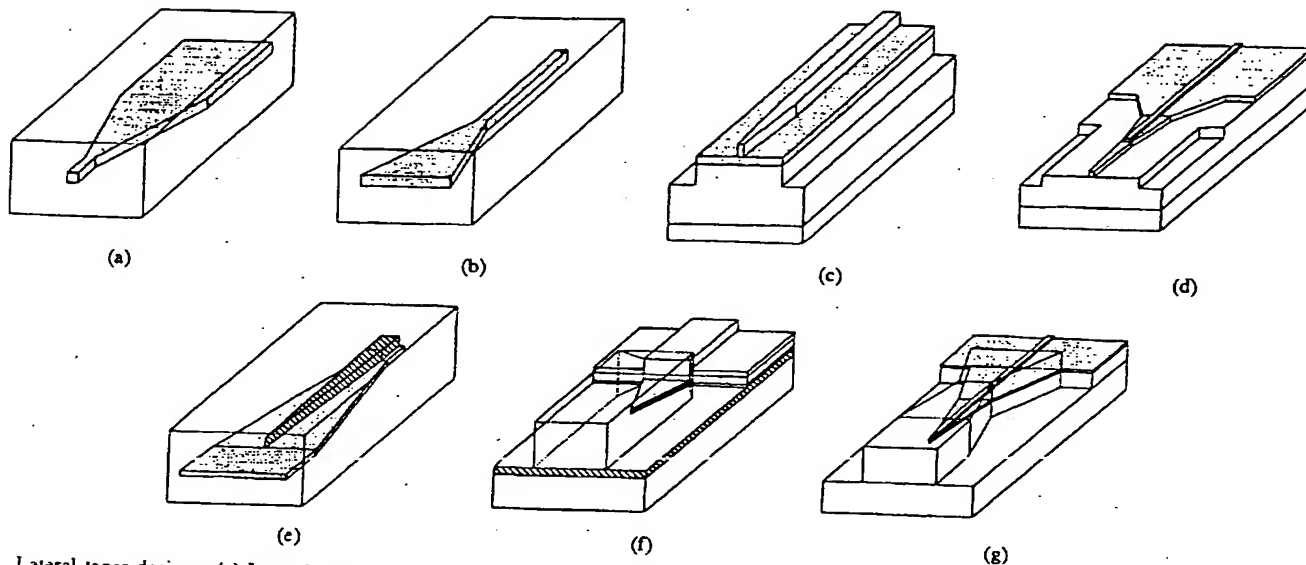
Fig. 2. Lateral taper designs. (a) Lateral down-tapered buried waveguide. (b) Lateral up-tapered buried waveguide. (c) Single lateral taper transition from a ridge waveguide to a fiber-matched waveguide. (d) Multisection taper transition from a ridge waveguide to a fiber-matched waveguide. (e) Dual lateral overlapping buried waveguide taper. (f) Dual lateral overlapping ridge waveguide taper. (g) Nested waveguide taper transition from a ridge waveguide to a fiber-matched waveguide.

transition region, in which one or both of the waveguides can be tapered. It is important that the taper angle in the transition region is sufficiently small, to prevent coupling of power from the fundamental mode into the higher order taper modes. The waveguide near the end facet is often fiber matched (e.g., a homostructure or diluted waveguide). In such an overlapping waveguide structure, it is possible to change the vertical waveguide structure, just by changing the lateral dimensions along the tapered section and without changing layer thicknesses.

In Fig. 2(c) a narrow and thin-ridge waveguide is transferred into a wide and thick ridge waveguide by means of a single lateral overlapping waveguide taper [19]. The ridge waveguide at the end of the taper can be a fiber-matched waveguide. In the tapered section, the width of the upper ridge is sufficiently decreased so that the optical mode in the upper ridge is in cutoff near the taper facet and only a wide optical mode, defined by the lower ridge, is supported. In this way, the strongly confined optical mode will expand into a weekly confined one. Since the upper ridge waveguide has to be in cutoff at the taper facet, the upper ridge needs to be tapered to rather small dimensions (<1 μm) and, hence, requires an accurate pattern definition and a controlled etching process. Despite the critical processing, the fabrication is simple, as no growth is required. A similar design is presented in Fig. 2(d) [20]. The difference is that the taper is split-up in several sections.

A Fig. 2(e), a very popular approach is given for changing both lateral and vertical dimensions of a buried waveguide by dual lateral overlapping waveguide taper [21]. The width of the upper waveguide becomes continuously smaller along the taper terminating in a very narrow end, whereas the width of the lower waveguide increases along the taper. This type of taper design has been applied by many researchers and

has proven to be very successful (see Sections IV and V). By a proper selection of the composition and thickness of both composing waveguides, the dual lateral overlapping buried waveguide taper can be compatible with a lot of optoelectronic components. A disadvantage of this type of taper, is the need for a sharp termination point of the upper waveguide, which complicates the taper fabrication process.

Zengerle has made a comparison, both experimentally and theoretically, between a simple laterally down-tapered waveguide and a dual lateral overlapping buried waveguide taper [21]. It seems that for the dual lateral taper the coupling loss is slightly lower and that the fabrication tolerances are much less stringent.

The taper design of Fig. 2(f) is not much different from the previous design: instead of a buried waveguide, a ridge waveguide is laterally tapered from a narrow ridge with a thick strongly guiding layer, to a wide ridge with a thin weekly guiding layer [22]–[24].

In the last taper design of Fig. 2, the incoming narrow rib waveguide is converted into a fiber-matched rib waveguide by means of two nested waveguide tapers [25]. The maximum coupling efficiency that be achieved is limited by the quality of the taper tips and such taper design therefore requires high resolution fabrication technologies.

C. Vertical Tapers

In a vertical taper, the thickness of the guiding layer(s) is changed along the device. In contrast to lateral tapers, where standard processing techniques can be used for the definition of the taper, special growth and etching techniques are required to change the thickness along the taper. A wide variety of technologies have therefore been developed to gradually change the thickness of a guiding layer (see Section III).
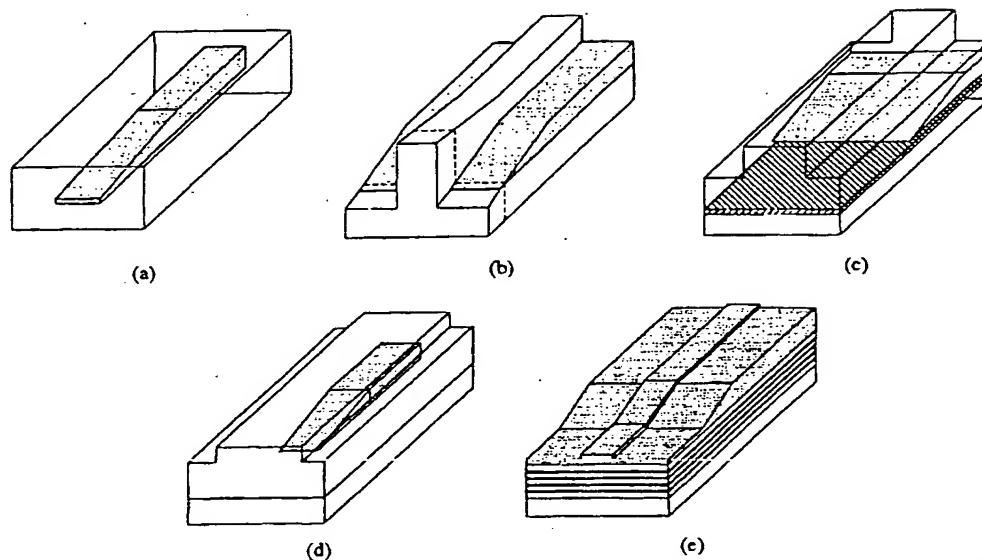
Fig. 3. Vertical taper designs. (a) Vertical down-tapered buried waveguide. (b) Vertical down-tapered ridge waveguide. (c) Vertical overlapping ridge waveguide taper. (d) Vertical overlapping waveguide taper transition from a buried waveguide to a fiber-matched waveguide. (e) Vertical overlapping waveguide taper transition from a ridge waveguide to a fiber-matched waveguide.
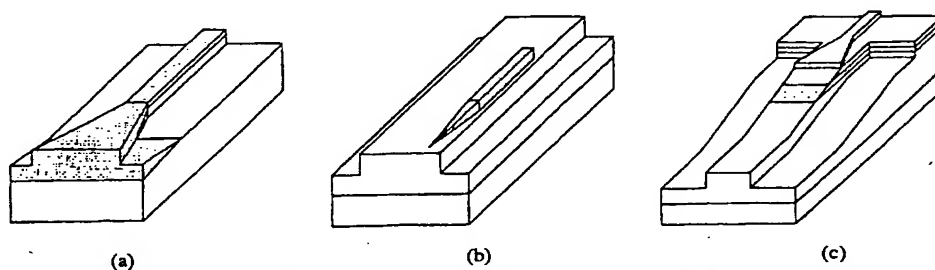
Fig. 4. Combined vertical and lateral taper designs. (a) Combined lateral and vertical ridge waveguide taper. (b) 2-D overlapping waveguide taper transition from a buried waveguide to a fiber-matched waveguide. (c) Overlapping waveguide taper transition with two sections from a ridge waveguide to a fiber-matched waveguide.

Examples of one dimensional vertical tapers are given in Fig. 3(a) for a buried waveguide structure [26] and in Fig. 4(b) for a ridge waveguide structure [27]. A facet needs to be cleaved at the position of the dashed line in Fig. 3(b).

Also for vertical tapers there exist several designs which make use of overlapping waveguides. In Fig. 3(c) [28], [29], tapering is achieved by reducing the thickness of the upper guiding layer until the upper guiding layer has completely disappeared near the end facet. Although this design has a ridge structure all over the taper, epitaxial regrowth is needed after taper definition.

In Fig. 3(d), a small spot-size buried waveguide is transformed into a large spot-size fiber-matched waveguide by means of a wedge-shaped vertical taper [12]. Also in this design, the lateral dimensions of the waveguide are changed: a narrow (buried) waveguide is converted to a wide (fiber-matched ridge) waveguide, simply by vertically tapering the buried guiding layer.

In Fig. 3(e), the thickness of the upper guiding layer is vertically down-tapered and provided with a rib of constant width and height. At the beginning of the taper the mode is vertically guided by the upper guiding layer, while along the taper, the mode expands vertically into the thin guiding layers

of the diluted fiber-matched structure. As the coupling loss is strongly dependent on the thickness of the residual upper guiding layer, the only critical issue for the taper fabrication is the thickness control of the tapered waveguide. The other processing steps are rather simple, since neither epitaxial regrowth, nor deeply etched ridges are necessary.

D. Combined Tapers

In a combined taper, both the lateral and the vertical dimensions of the guiding layer(s) are changed. Fig. 4(a) shows a design in which both the thickness and the width of a ridge waveguide are up-tapered toward the end facet [30]. Generally the thickness of a guiding layer is reduced to spread the optical mode, resulting in a waveguide which operates near cutoff. In this design the thickness of the guiding layer is increased, leading to a multimode waveguide. When the taper is adiabatic, the intermode coupling is minimal and the waveguide at the end facet behaves single-mode. The main advantage of a thick guiding layer at the large spot-size end of the taper, is the improved fabrication tolerances compared to a thin guiding layer.

The design is Fig. 4(b) is a two-dimensional (2-D) overlapping waveguide taper transition from a buried waveguide
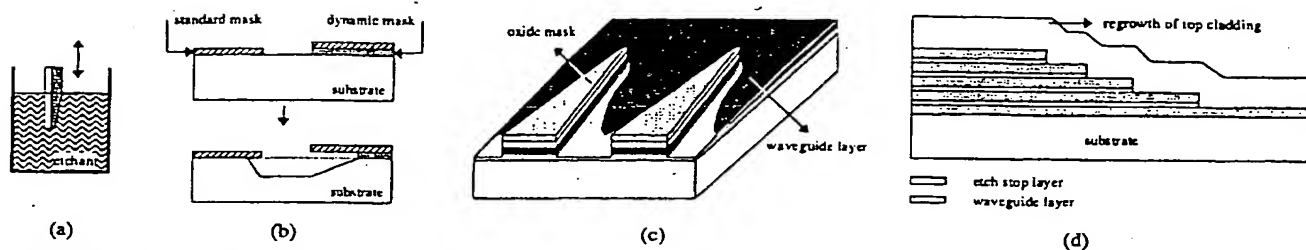
Fig. 5. Taper fabrication methods based on wet etching. (a) Dip-etch technique. (b) Dynamic etch mask technique. (c) Stepped etching. (d) Diffusion-limited etch technique.

to a fiber-matched waveguide [13]. Another two-dimensional overlapping waveguide taper design is illustrated in Fig. 4(c), where a ridge waveguide is transformed in a fiber-matched waveguide [31]. Fig. 4(b) and (c) are only a few examples, there exist more designs. Although very low coupling efficiencies have been demonstrated, most of these 2-D overlapping waveguide tapers are rather complex and therefore require a considerable number of fabrication steps, of which some can be very critical.

E. Special Tapers

There also exist alternative taper designs which cannot be simply classified in lateral, vertical or combined tapers. One such design is the waveguide coupler, which consist of one guiding layer in the small spot section and two rather closely spaced guiding layers in the large spot section [32]. The lower guiding layer is continuous throughout the device, whereas the transition from one to two guiding layers is abrupt. Perhaps this design could be classified as vertical overlapping waveguide taper with a "zero" taper length. When light is propagating from the one layer section to the two layer section, it is partly coupled into the upper waveguide. The spot-size at the output facet is maximized by optimizing the length of the two layer section. In this way, very short tapers (typically 20 μm) have been realized using a simple fabrication process. This design is however less flexible and only allows a limited enlargement of the spot size.

A second alternative design we would like to mention is a waveguide structure in which the beam size can be controlled by injecting current in a twin-stripe region [33]. A lateral waveguide is formed by the inner stripe, were no current is injected, between two stripes, where current is injected. The higher current density under the stripes results in a lower refractive index. The lateral refractive index profile, and thus the beam size, is influenced by injecting current. A laser diode with a beam size ratio of more than 2 has been demonstrated. Laser diodes with a variable beam size have no real applications in optical fiber-networks, but can be very promising for laser printers, where the size of the dots is electrically varied.

III. FABRICATION METHODS

L Introduction

We have observed in Section II that some taper structures have a simple design, others have a rather complicated struc-

ture. There exist nearly as much fabrication methods as there are taper designs.

The fabrication of a lateral taper is rather straightforward and can generally be done using standard processing techniques. Laterally tapers can be achieved by standard photolithography followed by wet chemical etching or dry etching. Possible dry etching techniques are: reactive ion etching (RIE), reactive ion beam etching (RIBE), N_2 ion milling ... Standard photo lithography does not allow to define very fine structures. Sharp taper tips are usually defined by electron beam (e-beam) writing in combination with a dry etching technique. The e-beam writing method offers a high spatial resolution, but is expensive and time-consuming when large areas have to be written. In order to prevent e-beam writing, the "knife-edge" technique can also be used for the definition of sharp tips [34]. The taper is formed by two "knife edge"-like photolithographic masks. After each (standard) photolithographic step one side of the taper is etched.

For vertical tapers, a lot a technologies have been developed. For the discussion of the different technologies, a classification is made between etching, growth and disordering techniques.

B. Etching Techniques

The most straightforward technology to realize a vertical taper is the *dip-etch process* [28]. The waveguide taper is etched by dipping it in a controlled way into the etchant [see Fig. 5(a)]. This etch technique is simple, but leads generally to fairly long tapered structures. Furthermore, it is impossible to process a full wafer.

A second wet etch technique is the *dynamic etch mask technique* [35]. The semiconductor is first covered with a thin-film material, which forms the dynamic mask and whose etch rate is significantly higher than the etch rate of the semiconductor material [see Fig. 5(b)]. This dynamic mask just covers the area where the taper is desired. The upper etch mask (e.g., photoresist or oxide) is subsequently deposited over the entire sample. This mask is opened near the dynamic mask at the place where the deeply etched end of the taper is desired. The taper is then chemically etched. Due to the high etch rate of the dynamic mask, more and more semiconductor material will be exposed to the etchant during etching. Taper structures with a length of only 50 μm have been realized in this way.

A third wet etch technique to realize vertical tapering is the *diffusion limited etch technique* [27]. By partially covering
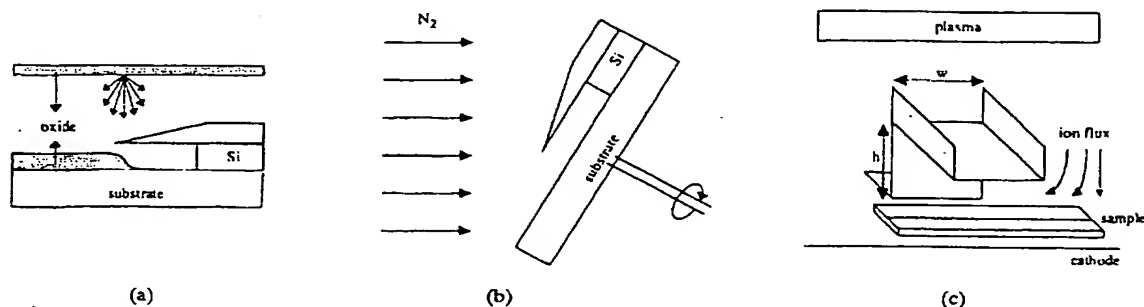
Fig. 6. Taper fabrication methods based on dry etching. (a) Oxide shadow technique. (b) Direct shadow etching. (c) Shadow masked reactive ion etching.

the substrate with a SiO_x-mask and using a diffusion-limited wet etchant, the etch rate can be controlled laterally over the substrate [see Fig. 5(c)]. For narrower mask openings, enhanced etch rates are obtained.

The main disadvantages of previous wet etch techniques are the low reproducibility and the difficulty to define sophisticated taper profiles such as parabolic or exponential shapes. Nonlinear taper profiles are, however, often recommended for reducing the taper length [36].

A wet etch technique that allows more reproducible tapered profiles, is the reduction of the thickness of the waveguide core by *stepped etching* [13], [37], [38]. Several etch-stop layers are embedded within the guiding layer, in order to form a staircase profile by sequentially displaced masking and selective etching [see Fig. 5(d)]. A sufficient number of steps is required to allow adiabatic mode expansion. This technique is again quite simple, but time consuming, since a lot of photolithographic and etching steps are needed.

There also exist several dry etching techniques for realizing vertical taper profiles. They all make use of shadow masks. The first technique described is the *oxide shadow etching* technique. A shadow mask made of silicon is fixed above the substrate on top of a spacer in a sputter chamber [see Fig. 6(a)] [39]. First, a tapered oxide layer is deposited on the substrate. Afterwards this oxide profile is transferred into the semiconductor by N_2 ion milling. The taper profile is controlled by the shape of the shadow mask.

A similar dry etch technique is the *direct shadow etching* technique. Again a silicon shadow mask is fixed above the substrate on top of a spacer. In contrast to the shadow etching technique, the substrate with shadow mask is placed directly in a N_2 ion milling module, with the axis of rotation tilted with respect to the direction of the ion beam [see Fig. 6(b)] [39]. After etching, a tapered transition is observed in the semiconductor. The taper profile is now controlled by the tilt angle and the height of the spacer of the shadow mask. An evaluation of the oxide shadow etching and direct shadow etching techniques has shown that both techniques are simple and reproducible, and allow a precise definition of the taper profile.

Finally, a vertical taper can also be achieved by placing a shadow mask above the substrate in a RIE system [29]. During *shadow masked RIE*, the taper length is mainly determined by the spacing (h) of the shadow mask with respect to the substrate.

The dry etching techniques are very successful for realizing single tapered devices or arrays of tapered devices, but do not easily allow the processing of a full wafer with a high density of tapers.

C. Epitaxial Growth Techniques

Vertical tapers can also be formed in situ during epitaxial growth, so that, in contrast with most wet or dry etching techniques, guiding layer and top cladding layer can be grown in a single growth step.

During molecular beam epitaxy (MBE) growth of AlGaAs, it is possible to obtain spatial variations in growth rate and composition by introducing a *temperature gradient* across the substrate, e.g., by using a mounting block whose top surface is slightly recessed in several regions [see Fig. 7(a)] [40], [41]. Above 650 °C the sticking coefficient of Ga decreases continuously with increasing temperature. Growing at temperatures above 650 °C, will therefore result in a spatial gradient in thickness and composition. When growing at lower temperatures, the sticking coefficient is insensitive to growth-temperature variations and the growth is uniform. Cladding layers are therefore grown at low temperatures, while the temperature is increased for the growth of the guiding layer. Both thickness and compositional variations result in a weaker confinement in the taper. The change in refractive index (due to the compositional change) accounts for 75% of the reduction in the vertical far-field beam divergence, while the change in vertical dimensions accounts for the remaining 25% of the reduction.

Another *in situ* technique is the *growth on a ridge*. Due to the mass transport properties of liquid phase epitaxy (LPE)-growth [6] and the surface diffusion properties of metal–organic vapor phase epitaxy (MOVPE)-growth [42], the growth rate on a ridge is dependent on the width of the ridge. During LPE the growth rate decreases [see Fig. 7(b)], whereas during MOVPE the growth rate increases as the width of the ridge decreases [see Fig. 7(c)].

Similar to the diffusion-limited etch technique, the growth rate in a MOVPE process will be enhanced when the substrate is covered by a dielectric mask, since no deposition takes place on the dielectric mask [see Fig. 7(d)] [30]. This technique is better known as the *selective area growth* (SAG) technique. The larger the mask width, the smaller the mask window and the higher the reactor pressure, the larger the growth rate enhancement [43]. The taper in Fig. 3(b) is actually realized
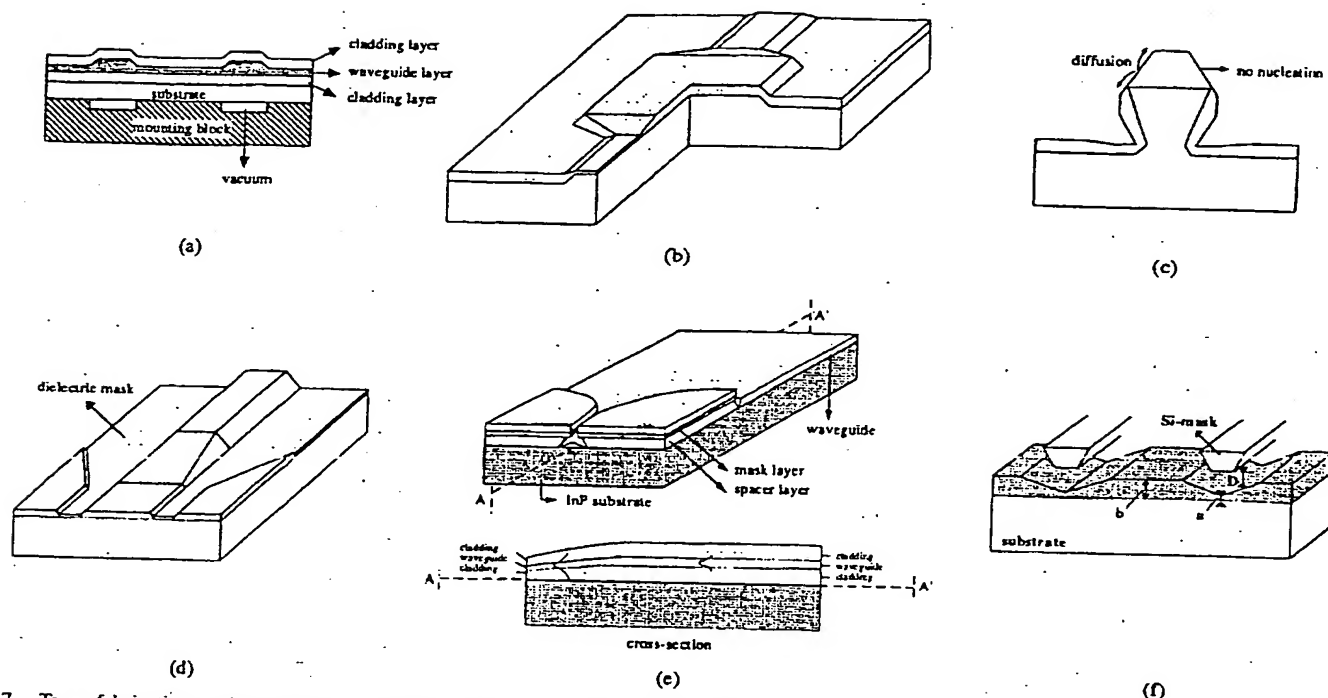
Fig. 7. Taper fabrication methods based on epitaxial growth. (a) Temperature gradient during MBE. (b) LPE-growth on a ridge. (c) MOVPE-growth on a ridge. (d) selective area growth. (e) Shadow masked growth with monocrystalline mask. (f) Shadow masked growth with mechanical shadow mask.
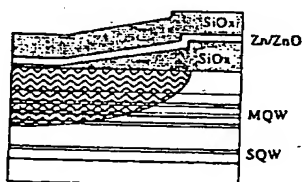

Fig. 8. Impurity-induced layer disordering (IILD).

by the diffusion-limited etching of the guiding layer, followed by the selective area growth of the cladding-layer using the same SiO_x-mask. In this way the thickness of the cladding layer will increase as the optical mode size increases.

With the SAG-technique it is also possible to realize a vertical taper by butt-joint coupling [44], [45]. First the device layers are grown. Then the substrate is partially covered by a dielectric mask, only leaving the taper region unmasked. The device layers are removed in the unmasked area (or taper region) by etching. Finally, a selective regrowth is performed to form the taper. As the growth rate is enhanced close to the dielectric mask, the regrown layers will be vertically tapered, with decreasing thicknesses away from the butt-joint. This technique requires at least one regrowth. Generally a second growth is done for the growth of the cladding layers. The formation of the butt-joint in the first regrowth is a rather critical process and requires an extensive growth optimization. The main advantage of the butt-joint is its flexibility to separately design the device layers and the taper layers.

The last in situ technique we would like to describe is the *shadow masked growth* (SMG) technique, which has been developed at our laboratory [46]. SMG uses a *monocrystalline mask*, which is held by means of a spacer layer at a certain distance above the substrate [see Fig. 7(e)]. During MOVPE epitaxial growth the deposition on the substrate takes place through the window in the shadow mask. Thickness changes are fully controlled by the lateral dimensions of the shadow mask and the reactor pressure: the smaller the mask window and the higher the reactor pressure, the larger the growth rate reduction relative to the nominal growth rate on a nonmasked substrate. A drawback of the SMG-technique is the additional growth step of the shadow mask and an additional processing step to remove the shadow mask. However, this drawback might be eliminated by using a mechanical mask instead of a monocrystalline mask, e.g., a silicon mask [47]. This *mechanical mask* is then placed on top of the substrate and can be easily removed after epitaxial growth [see Fig. 7(f)]. The SMG technique with mechanical mask has also been applied with MBE-growth [48].

SMG and SAG are very similar techniques. During SMG the growth rate decreases, while during selective area growth the rate increases. Both techniques show not only thickness variations, but also compositional variations [46], [49]. In both cases, tapering is the result of the cooperation between thickness reduction and compositional changes. In most tapered devices the thickness of the waveguide layer is decreased near the end of the taper. For this reason the SMG-technique is advantageous to the selective area growth technique. The nominal (uniform) waveguide layer can be grown on the nonmasked part of the substrate during SMG, enabling high quality layers. On the contrary, the nominal waveguide layer must be grown selectively when using the SAG technique.

TABLE I
OVERVIEW OF TAPERED WAVEGUIDE PERFORMANCES

Group	Technology	λ (nm)	C.L. (dB)	Align. Tol. (±) L (μm)	Align. Tol. (±) V (μm)	Remarks	Ref.
• Multisection taper from a ridge to a fibre-matched waveguide (Fig. 2.d)							
Siemens	RIE	1550	< 3.3 (CF) *	4 (1 dB)	2 (1 dB)	WG/PIN-diode	20
• Dual lateral overlapping buried waveguide taper (Fig. 2.e)							
Deutschen Telek.	Direct e-beam writing + RIE + regrowth	1550	<1.4 (CF) *			linear taper	21
Deutschen Telek.	Direct e-beam writing + RIE + regrowth	1550	<1.1 (CF) *			non-linear taper	21
AT&T	Knife-edge litho + selective etching + regrowth	1550	2.3 (CF)			AR-coating Electroabsorption modul.	53
• Dual lateral overlapping ridge waveguide taper (Fig. 2.f)							
NTT	Cl₂ RIBE + SAG regrowth of upper cladding	1550	3.5 (CF) *	2.5 (1 dB)	1.9 (1 dB)	AR-coating Phase-modulator device	22
NTT	Cl₂ RIBE + SAG (?) regrowth of upper cladding	1550	2.3 (CF) *			AR-coating Optical switch	23
• Nested taper from a ridge to a fibre-matched waveguide (Fig. 2.g)							
ANT	Standard litho + RIE + regrowth	1300-1550	4 (CF)			no AR-coating	25
• Vertical down-tapered ridge waveguide (Fig. 3.b)							
ETHZ	Diffusion limited etching + SAG regrowth	1530	0.9 (LF) *			AR coating	27
ETHZ	Diffusion limited etching + SAG regrowth	1530	1 (CF) *	2.5 (1 dB)	2.5 (1 dB)	AR coating	54
Our work	SMG + wet etching of ridge	1550	1.7 (LF) *	1.2 (1 dB)	1.2 (1 dB)		55
• Vertical down-tapered slab waveguide							
MIT Lincoln Lab	Temperature gradient during MBE	880				vertical beam width: 8.2°	40, 41
— Vertical overlapping ridge waveguide taper (Fig. 3.c)							
ETHZ	Dip etch + regrowth	1530	1.7 (LF)	0.8 (1 dB)	0.8 (1 dB)	AR-coating	28
Deutschen Telek.	Shadow masked RIE + regrowth	1550	< 2.8 (CF)	1.7 (1 dB)	1.5 (1 dB)	no AR-coating	29
• Vertical overlapping waveguide taper from a ridge to a fibre-matched waveguide (Fig. 3.e)							
HHI	Shadow masked RIE, no regrowth	1550					57
• Vertical overlapping waveguide taper from a buried to a fibre-matched waveguide (Fig. 3.d)							
Siemens	Oxide shadow etching + regrowth	1550	< 2 (CF)	3 (1 dB)	2.1 (1 dB)	AR-coating	12, 56
• Combined lateral and vertical ridge waveguide taper (Fig. 4.a)							
Bellcore	SAG (vertical), RIE (lateral)	1540	3 (CF) *				30
• 2-D overlapping waveguide taper from a buried to a FM waveguide							
NTT	Stepped etching (vertical taper) + Cl₂ chemical dry etching (lateral taper) + regrowth	1550	0.4 (CF) *	2.7 (1 dB)			13
• 2-D overlapping waveguide taper from a ridge to a FM waveguide							
CNET	RIE/stepped etching (vertical) + regrowth standard litho/RIE (lateral)	1550	4.5 (CF)	2.8 (1 dB)	2 (1 dB)	Polarization independent	58
• 2-section 2-D overlapping waveguide taper from a ridge to a FM waveguide (Fig. 4.c)							
Siemens	Direct shadow etching (vertical), standard litho + IBE + wet selective etching (lateral)	1550	1.5 (CF)	4 (3 dB)	3 (3 dB)	Optical switch	31, 59
• Waveguide coupler							
GMMT	Wet selective etching of upper WG + RIE (ridge)	1545	7.4 (CF) 1.7 (LF)				32

* including taper loss
CL: coupling loss
FM: fiber-matched
MBE: molecular beam epitaxy
SAG: selective area growth

2-D: two-dimensional
CF: cleaved single-mode fiber
HR: high-reflective
RIE: reactive ion etching
SMG: shadow masked growth

AR: antireflective
litho: photolithography
LF: lensed fiber
(R)IBE: (reactive) ion beam etching
SQW: single-quantum well

TABLE II
OVERVIEW OF TAPERED LASER DIODE PERFORMANCES

Group	Technology	λ (nm)	Type	I_{th} (mA)	QE (%)	CL (dB)	Align. Tol. (±) L (μm)	V (μm)	Remarks	Ref.
Laterally down-tapered buried waveguide (Fig. 2.a)										
NTT	Direct e-beam writing + RIE	1550	DH, DBR BH	9	21	2.8 (CF)	2 (1 dB)	2 (1 dB)	Beam divergence: 12°x12°	16
NTT	Stepper litho + RIE	1300	DH, PBH	4.7	57	2.3 (CF)	2.8 (1 dB)	3.2(1 dB)	HR-coating High temp.: 85°	60
AAR	Standard litho + chemical undercut of SiO2-mask + RIE (no stair case profile)	1480	MQW, BRS	25	52	1.4 (LF) 5.2 (CF)			HR-coating Beam divergence: 13°x15°	61
Matsushita	Conventional PBH technology (Lateral taper over whole cavity)	1300	MQW, PBH	6.9	65	4	1.7 (1 dB)	1.7 (1 dB)	HR-coating Beam divergence: 13°x13°	62
NEC	Chemical etching	1300	MQW, PBH	3	63	6.2 (CF)	2 (1 dB)		HR-coating Beam divergence: 14°x16°	63
Laterally up-tapered buried waveguide (Fig. 2.b)										
MIT Lincoln Lab	Selective chemical etching	1300	DH, PBH						Cylindrical mirror facets Lateral divergence: 9°	17
Hitachi		980	SQW, BR	20 mA					High power: 430 mW	64
Laterally up-tapered slab waveguide										
MIT Lincoln Lab	Tapered contact + etched cavity spoiling grooves	1300	SCH, MQW	1000	30				High power: 0.5 W (3A) Lateral divergence: 0.43°	65
MIT Lincoln Lab	Tapered contact + etched cavity spoiling grooves	980	GRINSCH	500	64				High power: 4.2 W (10A) Lateral divergence: 0.36°	66
Single lateral taper from a ridge to a FM-waveguide (Fig. 2.c)										
Sandia NL	Direct e-beam writing + Cl2 RIBE (standard litho also possible)	980	GRINSCH ridge	110	19.8	0.9 (CF)			Beam divergence: 5.6°x7.4°	19
Hitachi	Standard litho + wet etching	1300	MQW, ridge	25	62	4.8 (CF)	2.4 (1 dB)	1.5 (1 dB)	HR-coatings Beam divergence: 5.4°x19°	67
Hitachi	Standard litho + wet etching	980	DQW, ridge	19	63				Beam divergence: 10°x15° High power: 390 mW	68
Dual lateral overlapping buried waveguide taper (Fig. 2.e)										
Deutschen Telek.	Direct e-beam writing + RIE + regrowth	1530	DFB, MQW Mushroom	40	14.8	1.85 (CF) 0.9 (C DSF)	2.35 (1 dB)	2.15 (1 dB)		69
NTT	Stepped litho + Cl2 RIBE + SAG regrowth of upper cladding. 2" wafer processing	1300	DH, BH	21.4	26.2	2.4 (CF)	2 (1 dB)	2 (1 dB)	Beam divergence: 7° x 11°	24, 70
AT&T	Knife-edge litho + selective etching + regrowth	1550	MQW, PBH	12	52	3.5 (CF)	3.1 (1 dB)	2.6 (1 dB)	Beam divergence: 5° x 7°	34
AT&T	Knife-edge litho + selective etching + regrowth	1300	MQW, PBH	22	51	3.5 (CF)	2.8 (1 dB)	2.5 (1 dB)	Beam divergence: 6° x 8°	34
Furukawa	Wet chemical etching + regrowth	1300	MQW, PBH	14	45				Beam divergence: 10°x11°	71
BTL	Wet chemical etching	1560	MQW, PBH	12		4.6 (CF)			Beam divergence: 15°x15°	72
BTL	Wet chemical etching 2" wafer processing	1550	MQW, PBH			1.8 (CF)	5.5 (3 dB)	3.5 (3 dB)	Beam divergence: 5.5°x10°	73, 74
CSELT	2-steps litho + RIE etching (in situ etch depth control)	1550	MQW, BR	30	21	2.2 (CF)	2.3 (1dB)	2.15 (1dB)	Beam divergence: 6.6°x11°	75

D. Disordering

The last technique that will be reviewed is *impurity-induced layer disordering* (IILD) [50]. By Zn-diffusion through a tapered SiO_x barrier (see Fig. 8), the ions in a multiquantum well (MQW) are intermixed, so that the quantum wells are gradually destroyed. As a result, the bandgap of the destroyed MQW increases, which means that the refractive index of the MQW-region decreases. This technique is suitable for interconnecting a MQW-waveguide to a single QW-waveguide. This technique eliminates the need for regrowth in the fabrication process, but it appears to be very difficult to optimize and to reproduce the diffusion profile.

IV. TAPERED WAVEGUIDE PERFORMANCES

In Table I, an overview is given of tapered waveguides realized by different research groups. The devices are classified according to their taper designs as discussed in Section II. The first column indicates the research group. The second column shows the applied fabrication technology. The third column contains the wavelength of the guided light. The next columns summarize the taper performances, such as the fiber-chip coupling loss to a single mode cleaved fiber (CF) or lensed fiber (LF), the lateral (L) and vertical (V) alignment tolerances. The value between brackets in the columns for the alignment tolerances, gives the excess loss corresponding to a lateral or vertical displacement. The last two columns contain some remarks and references.

Most of the tapered waveguides have been developed for an operating wavelength of 1.55 μm. The lowest coupling loss reported, is only 0.4 dB, which means that 91% of the light can be coupled into the cleaved fiber. In this case the (1 dB) alignment tolerances are close to 3 μm. This should be compared to untapered small spot-size waveguides which

TABLE II (Continued)
OVERVIEW OF TAPERED LASER DIODE PERFORMANCES

Group	Technology	λ (nm)	Type	I_{th} (mA)	QE (%)	CL (dB)	Align. Tol. (±) L (μm)	V (μm)	Remarks	Ref.
Vertical down-tapered buried waveguide (Fig. 3.a)										
NTT	SAG of butt-joint	1300	MQW, PBH	7	33.3	1.06 (CF)	2 (1 dB)	2 (1 dB)	1 HR-coating Beam divergence: 7° x 10°	45
NTT	SAG of butt-joint, 2" wafer processing	1300	MQW, PBH	5.6		0.94 (CF)	2 (1 dB)	2 (1 dB)	2 HR-coatings High power: 50 mW High temp.: 134°	44, 76
AT&T	Stepped etching	1500	MQW, PBH	28	17	5. (CF)	3 (1 dB)	2 (1 dB)	Beam divergence: 10°x15°	38
Mitsubishi	SAG	1550 ?	PBH			3.3 (CF)	3 (1 dB)	3 (1 dB)	Beam divergence: 11°x11°	77
Hitachi	Si SMG	1300	MQW, PBH	16	56	3.5 (CF)	2 (1 dB)	2 (1 dB)	Beam divergence: 12°x13° High temp.: 85°	47
Furukawa	SAG	1300	MQW, PBH	16	32				Beam divergence: 11°x11° High temp.: 120° High power (> 50 mW)	78
Fujitsu	SAG	1300	MQW, PBH	6.5	40	3.8 (CF)	2 (1 dB)	2 (1 dB)	HR-coating Beam divergence: 9°x11°	79
Our work	SMG	1550	MQW, PBH	8.2	31.5	3.3 (CF) 1.7 (LF)	2.1 (1 dB) 1.3 (1 dB)	1.7 (1 dB) 1 (1 dB)	Beam divergence: 12°x16°	26
GMMT/Our work	SMG	1550	MQW, DFB PBH	10	34.7	5.3 (CF)	3.5 (1 dB)	1.5 (1 dB)	Beam divergence: 12°x14°	80
Vertical down-tapered ridge waveguide (Fig. 3.b)										
ETHZ	Diffusion limited etching + wet etch of ridge (including lateral taper)	1300	DH, ridge	55	8.5	3 (CF)	1.8 (1 dB)	1.8 (1 dB)		51
Mitsubishi	LPE-growth on ridge	780	DH, BTRS	60	42				AR-HR coating Beam divergence: 9°x10°	6
Our work	SMG	980	SQW, ridge	11.2	36				Beam divergence: 15°x29°	81
Vertically down-tapered and laterally up-tapered buried waveguide										
AT&T	Stepped etching (vertical) Wet etching (lateral)	1500	MQW, DBR PBH	52	30	4.2 (CF)	3.8 (1 dB)	2.1 (1 dB)	HR-coating Beam divergence: 12°x12°	37

AR: antireflective
C DSF: cleaved dispersion shifted fiber
DBR: distributed Bragg reflector
DQW: double-quantum well

HR: high-reflective
MQW: multiquantum well
RIBE: reactive ion beam etching
SQW: single-quantum well

BR(S): buried ridge (stripe)
CF: cleaved single-mode fiber
DFB: distribute feedback
(GRIN)SCH: (GRaded INdex) separate confinement heterostructure
LF: lensed fiber
(P)BH: (planar) buried heterstructure
SAG: selective area growth
temp.: temperature

BTRS: buried twin-ridge substrate structure
CL: coupling loss
DH: double heterostrucutre
FM: fiber-matched

litho: photolithography
QE: differential quantum efficiency
SMG: shadow masked growth

have coupling losses of typically 10 dB (only 10% of the light can be coupled into the fiber) and alignment tolerances around 1 μm. Some tapers have also been developed for coupling light into a lensed fiber. As expected, low coupling losses can be obtained, but the alignment tolerances do not really improve compared to untapered waveguides.

Several research groups achieve coupling losses around 1 dB, including taper loss (= spot-size conversion loss), which means that taper losses can be kept very low, which in turn indicates that the tapers are well designed and the fabrication technologies well established.

If we look at the performances of the dual lateral overlapping buried waveguide tapers of Deutschen Telekom with different taper profiles, then it is evident that improved performances are obtained with the (optimized) nonlinear taper.

From Table I, it is clear that a wide variety of taper designs have been investigated, but that only a few have really been integrated with an optoelectronic device (e.g., an optical switch, an electroabsorption modulator, waveguide/PIN-diode, ...). Actually, the number of taper designs, that has been

integrated with devices is higher: some of the taper designs in Table II have indeed been integrated with laser diodes (see Section V).

V. TAPERED LASER PERFORMANCES

A similar overview as in previous section is given in Table II for the tapered laser diodes. Most columns in Table II give the same information as in Table I. Column 4 describes the type of laser. Columns 6 and 7 give the threshold current and the differential quantum efficiency of the laser diodes.

Please note that, although the ETHZ-laser [51] also contains a lateral taper, it is classified under the vertical down-tapered ridge waveguides, because the corresponding drawing [Fig. 3(b)] very well illustrates the structure of the taper.

Most laser devices are Fabry–Perot type lasers. However, a few distributed Bragg reflector (DBR) and distributed feedback (DFB) laser are also reported, which indicates that the integration of a taper is compatible with the more complicated fabrication processes of highly advanced laser diodes.

In contrast to the tapered waveguides (see Table I), few taper designs have been investigated. The laterally down-tapered buried waveguide, the dual lateral overlapping buried waveguide taper and the vertical down-tapered waveguide designs seem to be very attractive for the monolithic integration of tapers with laser diodes. NTT has made a comparison between the latter two designs [82]. For the vertical down-tapered waveguide design, they made a distinction between a butt-joint coupled and the SAG or SMG MQW taper. They conclude that all type of tapers achieve similar performances with respect to coupling loss and spot-size conversion loss. Minimal coupling and taper loss is obtained at smaller thickness reductions for the butt-joint coupled taper compared to MQW vertical taper (factor 3 compared to 3.5). For the same coupling and taper loss, the dual lateral overlapping waveguide taper can have a shorter taper length.

Most of the tapered laser diodes in Table II exhibit similar performances with respect to threshold current and quantum efficiency as conventional untapered lasers. Coupling losses around 3 dB can be easily obtained, which means that ca. 50% of the emitted power can be coupled into a cleaved fiber. The lowest coupling losses reported are around 1 dB (80% coupling efficiency).

The laser performances given in Table II also confirm that the integration of a taper is advantageous for high-power and high-temperature operation. Optical powers larger than 4.2 and 0.5 W are reported by MIT Lincoln Lab for lasers operating at 980 and 1300 nm, respectively. These high power lasers emit a single lateral spatial mode with a beam divergence of only a few tenths of a degree. The highest operation temperature (134°) is reported by NTT for a butt-jointed vertical buried tapered laser.

Finally, we would like to remark that the technologies for tapered laser diodes are quite well established, since a few groups (NTT, BTL) have reported 2-in wafer processing.

VI. CONCLUSION

During the past years a lot of attention has been paid to the monolithic integration of spot-size transformers with II–V semiconductor devices, in order to reduce the fiber-chip coupling loss and the packaging cost of OEIC's in future optical networks.

A lot of taper designs have been proposed and nearly as many fabrication technologies have been developed. Some of those technologies are simple and make use of low-cost equipment, but do not offer a high flexibility in taper design, a high-resolution taper definition or a high reproducibility. Other fabrication techniques, which are much more reproducible and allow fine and sophisticated taper profiles, are often more complex and time consuming or require expensive installations. The main requirement for large scale production of low cost devices, however, is the ability to 2-in wafer processing with a reasonable yield.

The research activities on tapered devices, in particular tapered laser diodes, are still expanding, and performances continues to improve. At the moment tapered waveguides can be fabricated with a coupling loss of 0.4 dB when coupled to

a cleaved fiber. The best tapered lasers show coupling losses around 1 dB and beam divergences below 10°.

REFERENCES

[1] N. Kalonji and J. Semo, "High efficiency, long working distance laser diode to single mode fiber coupling," *Electron. Lett.*, vol. 30, no. 11, pp. 892–894, 1994.

[2] H. M. Presby and C. A. Edwards, "Near 100% efficient fiber microlenses," *Electron. Lett.*, vol. 28, no. 6, pp. 582–584, 1992.

[3] Y. Shani, C. H. Henry, R. C. Kistler, K. J. Orlowsky, and D. A. Ackerman, "Efficient coupling of a semiconductor laser to an optical fiber by means of a tapered waveguide on Si," *Appl. Phys. Lett.*, vol. 55, no. 23, pp. 2389–2391, 1989.

[4] M. Yanagisawa, H. Terui, Y. Yamada, S. Suzuki, and K. Kato, "Low-loss fiber coupling to laserdiode using 2%-Δ silica-based mode-field converting waveguide," in *Tech. Dig. Fourth Microoptics Conf. Eleventh Topical Meet. Gradient-Index Optical Systems*, Kawasaki, Japan, 1993, pp. 294–297.

[5] J.-M. Cheong, J.-W. Seo, and Y.-K. Jhee, "High alignment tolerance coupling scheme for multichannel laser diode/singlemode fiber modules using a tapered waveguide array," *Electron. Lett.*, vol. 30, no. 18, pp. 1515–1516, 1994.

[6] T. Murakami, K. Ohtaki, H. Matsubara, T. Yamawaki, H. Saito, K. Isshiki, Y. Kokubo, A. Shima, H. Kumabe, and W. Susaki, "A very narrow-beam AlGaAs laser with a thin tapered thickness active layer (T^3-laser)," *IEEE J. Quantum Electron.*, vol. QE-23, no. 6, pp. 712–719, 1987.

[7] N. Bouadma, A. Ougazzaden, M. Kamoun, C. Kazmierski, and L. Silvestre, "1.3 μm InGaP/InAsP MQW lasers with large spot size and low loss fiber chip coupling fabricated by a standard buried heterostructure process," *Electron. Lett.*, vol. 32, no. 17, pp. 1582–1583, 1996.

[8] M.-H. Shih, F.-S. Choa, R. M. Kapre, W. T. Tsang, R. A. Logan, and S. N. G. Chu, "Alignment-relaxed 1.55 μm multiquantum well lasers fabricated using standard buried heterostructure laser processes," *Electron. Lett.*, vol. 31, no. 13, pp. 1058–1060, 1995.

[9] D. Vakhshoori, W. S. Hobson, H. Han, J. Lopata, G. E. Henein, J. D. Wynn, J. de Jong, M. L. Schnoes, and G. J. Zydzik, "980 nm spread index laser with strain compensated InGaAs/GaAsP/InGaP and 90% fiber coupling efficiency," *Electron. Lett.*, vol. 32, no. 11, pp. 1007–1008, 1996.

[10] A. Malag and W. Strupinski, "MOVPE-grown (AlGa)As double-barrier multiquantum well (BDMQW) laser diode with low vertical beam divergence," *J. Cryst. Growth*, vol. 170, pp. 408–412, 1997.

[11] I. Moerman, G. Vermeire, M. D'Hondt, W. Vanderbauwhede, J. Blondelle, G. Coudenys, P. Van Daele, and P. Demeester, "III–V semiconductor waveguiding devices using adiabatic tapers," *Microelectron. J.*, vol. 25, pp. 675–690, 1994.

[12] G. Müller, B. Stegmüller, H. Westermeier, and G. Wenger, "Tapered InGaAsP waveguide structure for efficient fiber-chip coupling," *Electron. Lett.*, vol. 27, no. 20, pp. 1836–1838, 1991.

[13] N. Yoshimoto, K. Kawano, H. Takeuchi, S. Kondo, and Y. Noguchi, "Spot size convertors using InP/InAlAs multi quantum well waveguides for low-loss singlemode fiber coupling," *Electron. Lett.*, vol. 28, no. 17, pp. 1610–1611, 1992.

[14] R. J. Deri, N. Yasuoka, M. Makiuchi, A. Kuramata, and O. Wada, "Efficient fiber coupling to low-loss diluted multiple quantum well optical waveguides," *Appl. Phys. Lett.*, vol. 55, no. 15, pp. 1495–1497, 1989.

[15] K. Kasaya, O. Mitomi, M. Naganuma, Y. Kondo, and Y. Noguchi, "A simple laterally tapered waveguide for low loss coupling to single-mode fibers," *IEEE Photon. Technol. Lett.*, vol. 5, pp. 345–347, Mar. 1993.

[16] K. Kasaya, Y. Kondo, M. Okamoto, O. Mitomi, and M. Naganuma, "Monolithically integrated DBR lasers with simple tapered waveguide for low-loss fiber coupling," *Electron. Lett.*, vol. 29, no. 23, pp. 2067–2068, 1993.

[17] J. N. Walpole, Z. L. Liau, L. J. Missaggia, and D. Yap, "Diode lasers with cylindrical mirror facets and reduced beam divergence," *Appl. Phys. Lett.*, vol. 50, no. 18, pp 1219–1221, 1987.

[18] J. N. Walpole, "Semiconductor amplifiers and lasers with tapered gain regions," *Optical and Quantum Electron.*, vol. 28, pp. 623–645, 1996.

[19] G. A. Vawter, R. E. Smith, H. Hou, and J. R. Wendt, "Semiconductor laser with tapered-rib adiabatic-following fiber coupler for expanded output-mode diameter, *IEEE Photon. Technol. Lett.*, vol. 9, pp. 425–427, Apr. 1997.

[20] J. G. Bauer, M. Schier, and G. Ebbinghaus, "High responsivity integrated tapered waveguide PIN photodiode," in *Proc. 19th Eur. Conf. Optical Communication (ECOC '93)*, Montreux, Switzerland, pp. 277–280.

[21] R. Zengerle, O. Leminger, W. Weiershausen, K. Faltin, and B. Hübner, "Laterally tapered InP-InGaAsP waveguides for low-loss chip-to-fiber butt coupling: A comparison of different configurations," *IEEE Photon. Technol. Lett.*, vol. 7, pp. 532–534, May 1995.

[22] Y. Yoshimoto, K. Kawano, Y. Hasumi, T. Takeuchi, S. Kondo, and Y. Noguchi, "InGaAlAs/InAlAs multiple quantum well phase modulator integrated with spot size conversion structure," *IEEE Photon. Technol. Lett.*, vol. 6, pp. 208–210, Feb. 1994.

[23] K. Kawano, M. Kohtoku, N. Yoshimoto, S. Sekine, and Y. Noguchi, "2 × 2 InGaAlAs/InAlAs multiquantum well (MQW) directional coupler waveguide switch modules integrated with spot size convertors," *Electron. Lett.*, vol. 30, no. 4, pp. 353–354, 1994.

[24] M. Wada, M. Kohtoku, K. Kawano, S. Kondo, Y. Tohmori, Y. Kondo, K. Kishi, Y. Sakai, I. Kotaka, Y. Noguchi, and Y. Itaya, "Laser diodes monolithically integrated with spot-size converters fabricated on 2 inch InP substrates," *Electron. Lett.*, vol. 31, no. 15, pp. 1252–1254, 1995.

[25] T. Schwander, S. Fischer, A. Krmer, M. Laich, K. Luksic, G. Spatschek, and M. Warth, "Simple and low-loss fiber-to-chip coupling by integrated field-matching waveguide in InP," *Electron. Lett.*, vol. 29, no. 4, pp. 326–328, 1993.

[26] I. Moerman, M. D'Hondt, W. Vanderbauwhede, P. Van Daele, P. Demeester, and W. Hunziker, "InGaAsP/InP strained MQW laser with integrated modesize converter using the shadow masked growth technique," *Electron. Lett.*, vol. 31, pp. 452–454, 1995.

[27] T. Brenner and H. Melchior, "Integrated optical modeshape adapters in InGaAsP/InP for efficient fiber-to-waveguide coupling," *IEEE Photon. Technol. Lett.*, vol. 50, pp. 1053–1056, Sept. 1993.

[28] T. Brenner, W. Hunziker, M. Smit, M. Bachmann, G. Guekos, and H. Melchior, "Vertical InP/InGaAsP tapers for low-loss optical fiberwaveguide coupling," *Electron. Lett.*, vol. 28, no. 22, pp. 2040–2041, 1992.

[29] B. Jacobs, R. Zengerle, K. Faltin, and W. Weiershausen, "Vertically tapered spot size transformers by a simple masking technique," *Electron. Lett.*, vol. 31, no. 10, pp. 794–796, 1995.

[30] R. J. Deri, C. Caneau, E. Colas, L. M. Schiavone, N. C. Andreadakis, G. H. Song, and E. C. M. Pennings, "Integrated optic mode-size tapers by selective organometallic chemical vapor deposition of InGaAsP/InP," *Appl. Phys. Lett.*, vol. 61, no. 8, pp. 952–954, 1992.

[31] G. Wenger, L. Stoll, B. Weiss, M. Schienle, R. Müller-Nawrath, S. Eichinger, J. Müller, B. Acklin, and G. Müller, "Design and fabrication of monolithic optical spot size transformers (MOST's) for highly efficient fiber-chip coupling," *J. Lightwave Technol.*, vol. 12, pp. 1782–1790, Oct. 1994.

[32] N. Shaw, P. J. Williams, J. Buus, "Optoelectronic integrated circuit (OEIC) waveguide coupler for spot size expansion and improved fiber coupling efficiency," *Electron. Lett.*, vol. 31, no. 14, pp. 1143–1145, 1995.

[33] S. Nakatsuka, S. Maruo, A. Arimoto, and S. Saitoh, "Laserdiode with controllable spot size ratio of 1 : 2.1," in *Pacific Rim Conf. Lasers and Electro-Optics Tech. Dig.*, 1995, p. 234, paper FU5.

[34] R. Ben-Michael, U. Koren, B. I. Miller, M. G. Young, M. Chien, and G. Raybon, "InP-based multiple quantum well lasers with an integrated tapered beam expander waveguide," *IEEE Photon. Technol. Lett.*, vol. 6, pp. 1412–1414, Dec. 1994.

[35] M. Chien, U. Koren, T. L. Koch, B. I. Miller, M. Oron, M. G. Young, and J. L. Demiguel, "Short cavity distributed bragg reflector laser with an integrated tapered output waveguide," *IEEE Photon. Technol. Lett.*, vol. 3, pp. 418–420, May 1991.

[36] G. R. Hadley, "Design of tapered waveguides for improved output coupling," *IEEE Photon. Technol. Lett.*, vol. 5, pp. 1068–1070, Sept. 1993.

[37] T. L. Koch, U. Koren, G. Eisenstein, M. G. Young, M. Oron, C. R. Giles, and B. I. Miller, "Tapered waveguide InGaAs/InGaAsP multiplequantum-well lasers," *IEEE Photon. Technol. Lett.*, vol. 2, pp. 88–90, Feb. 1990.

[38] G. Müller, G. Wender, L. Stoll, H. Westermeier, and D. Seeberger, "Fabrication techniques for vertically tapered InP/InGaAsP spot-size transformers with very low loss," in *Proc. Eur. Conf. Integrated Optics ECIO 93*, Neuchâtel, Switzerland, pp. 14–14.

[39] D. E. Bossi, W. D. Goodhue, M. C. Finn, K. Rauschenbach, J. W. Bales, and R. H. Rediker, "Reduced-confinement antennas for GaAlAs integrated optical waveguides," *Appl. Phys. Lett.*, vol. 56, no. 5, pp. 420–422, 1990.

[40] D. E. Bossi, W. D. Goodhue, L. M. Johnson, and R. H. Rediker, "Reduced-confinement GaAlAs tapered waveguide antennas for enhanced far-field beam directionality," *IEEE J. Quantum Electron.*, vol. 27, pp. 687–695, Mar. 1991.

[41] E. Colas, A. Shahar, and W. J. Tomlinson, "Diffusion-enhanced epitaxial growth of thickness-modulated low-loss rib waveguides on patterned GaAs substrates," *Appl. Phys. Lett.*, vol. 56, no. 10, pp. 955–957, 1990.

[42] G. Coudenys, G. Vermeire, Y. Zhu, I. Moerman, L. Buydens, P. Van Daele, and P. Demeester, "Novel growth techniques for the fabrication of photonic integrated circuits," in *Proc. Mater. Res. Soc. Symp.*, 1992, vol. 240, pp. 15–26.

[43] Y. Sakai, Y. Tohmori, Y. Suzaki, Y. Kondo, and O. Mitomi, "Improved FFP of 1.3 μm spot-size converted laser for highly efficient coupling to optical fiber," *Electron. Lett.*, vol. 32, no. 15, pp. 1372–1374, 1993.

[44] Y. Tohmori, Y. Suzaki, H. Fukano, O. Okamoto, Y. Sakai, O. Mitomi, S. Matsumoto, Y. Yamamoto, M. Fukuda, M. Wada, Y. Itaya, and T. Sugie, "Spot-size converted 1.3 μm laser with butt-jointed selectively grown vertically tapered waveguide," *Electron. Lett.*, vol. 31, no. 3, pp. 1069–1070, 1993.

[45] G. Coudenys, I. Moerman, Z. Q. Yu, F. Vermaerke, P. Van Daele, and P. Demeester, "Atmospheric pressure and low pressure shadow masked MOVPE growth of InGaAs(P)/InP and (In)GaAs/(Al)GaAs heterostructures and quantum wells," *J. Electron. Mater.*, vol. 23, no. 2, pp. 227–234, 1994.

[46] M. Aoki, M. Komori, M. Suzuki, H. Sato, M. Takahashi, T. Ohtoshi, K. Uomi, and S. Tsuji, "Wide-temperature-range operation of 1.3 μm beam expander-integrated laser diodes grown by in-plane thickness control MOVPE using a silicon shadow mask," *IEEE Photon. Technol. Lett.*, vol. 8, pp. 479–481, Apr. 1996.

[47] A. Lorke, J. H. English, A. C. Gossard, and P. M. Petroff, "Tapered GaAs quantum wells and selectively contactable two-dimensional electron gases grown by shadow masked molecular-beam epitaxy," *J. Appl. Phys.*, vol. 77, no. 7, pp. 3578–3580, 1995.

[48] I. Moerman, T. Van Caenegem, P. Van Daele, and P. Demeester, "MOVPE-based localized epitaxial growth techniques and its applications," in *Proc. Indium Phosphide and Related Materials Conf.*, Hyannis, MA, May 1997, pp. 610–613, paper ThD1.

[49] H. S. Kim, S. Sinha, and R. V. Ramaswamy, "An MQW-SQW tapered waveguide transition," *IEEE Photon. Technol. Lett.*, vol. 5, pp. 1049–1052, Sept. 1993.

[50] T. Brenner, R. Hess, and H. Melchior, "Compact InGaAsP/InP laser diodes with integrated mode expander for efficient coupling to flat-ended singlemode fibers," *Electron. Lett.*, vol. 31, no. 17, pp. 1443–1445, 1995.

[51] A. Shahar, W. J. Thomlinson, A. Yi-Yan, M. Seto, and R. J. Deri, "Dynamic etch mask technique for fabricating tapered semiconductor optical waveguides and other structures," *Appl. Phys. Lett.*, vol. 56, no. 12, pp. 1098–1100, 1990.

[52] U. Koren, R. Ben Michael, B. I. Miller, M. G. Young, M. Chien, H. H. Yaffe, G. Raybon, and K. Dreyer, "Electroabsorption modulator with passive waveguide spot size converters," *Electron. Lett.*, vol. 30, no. 22, pp. 1852–1853, 1994.

[53] T. Brenner, M. Bachman, and H. Melchior, "Vertically tapered InGaAsP/InP waveguides for highly efficient fiber-end single-mode fibers," *Appl. Phys. Lett.*, vol. 65, no. 7, pp. 798–800, 1994.

[54] I. Moerman, M. D'Hondt, W. Vanderbauwhede, J. Haes, L. Van Wassenhove, P. De Dobbelaere, R. Baets, P. Van Daele, P. Demeester, W. Hünziker, and C. Holtmann, "Vertically tapered InGaAsP/InP waveguides and lasers resulting in low-loss fiber-chip coupling," in *Proc. 20th Eur. Conf. Optical Communication (ECOC '94)*, Firenze, Italy, 1994, pp. 1027–1030.

[55] G. Wenger, G. Müller, B. Sauer, D. Seeberger, and M. Honsberg, "Highly efficient multi-fiber-chip coupling with large alignment tolerances by integrated InGaAsP/InP spot-size transformers," in *Proc. 18th Eur. Conf. Optical Communication (ECOC '92)*, Berlin, Germany, pp. 927–930.

[56] L. Möri, C. M. Weinert, F. Reier, L. Stoll, and H. P. Nolting "Uncladded InGaAsP/InP rib waveguides with integrated thickness tapers for efficient fiber-chip butt coupling," *Electron. Lett.*, vol. 32, no. 1, pp. 36–38, 1996.

[57] F. Ghirardi, B. Mersali, J. Brandon, G. Herve-Gruyer, and A. Carenco, "Quasi planar Spot-size transformer for efficient coupling between a cleaved fiber and an InP/InGaAsP rib waveguide," *IEEE Photon. Technol. Lett.*, vol. 6, pp. 552–524, Apr. 1994.

[58] G. Müller, L. Stoll, G. Wenger, and M. Schienle, "First low loss InP/InGaAsP optical switch with integrated mode transformers," in *Proc. 19th Eur. Conf. Optical Communication (ECOC '93)*, Montreux, Switzerland, pp. 37–40.

[59] H. Fukano, Y. Kadota, Y. Kondo, M. Ueki, Y. Sakai, K. Kasaya, K. Yokoyama, and Y. Tohmori, "1.3 μm large spot size laser diodes

with laterally tapered active layer," *Electron. Lett.*, vol. 31, no. 17, pp. 1439–1440, 1995.

[60] P. Doussiere, P. Garabedian, C. Graver, E. Derouin, E. Gaumont-Gaorin, G. Michaud, and R. Meilleur, "Tapered active stripe for 1.5 μm InGaAsP/InP strained multiple quantum well lasers with reduced beam divergence," *Appl. Phys. Lett.*, vol. 64, no. 5, pp. 539–541, 1994.

[61] Y. Inaba, M. Kito, T. Nishikawa, M. Ishino, and Y. Matsui, "Multiquantum-well lasers with tapered active stripe for direct coupling to single-mode fiber," *IEEE Photon. Technol. Lett.*, vol. 9, pp. 722–724, June 1997.

[62] A. Uda, K. Tsuruka, N. Suzuki, F. Fukushima, T. Nakamura, and T. Torikai, "Spot-size expanded high efficiency 1.3 μm MQW laser diodes with laterally tapered active stripe," in *Proc. Indium Phosphide and Related Materials Conf.*, Hyannis, MA, May 1997, pp. 657–660, paper ThF2.

[63] M. Sagawa, K. Hiramoto, T. Toyonaka, T. Kikawa, and K. Uomi, "High-power and highly-reliable operation of 0.98 μm lasers with an exponential-shapes flared stripe," in *Proc. 9th Annu. Meet. IEEE Lasers and Electro-Optics Soc.*, 1996, pp. 42–43, paper ME2.

[64] S. H. Grooves, J. P. Donnelly, J. N. Walpole, J. D. Woodhouse, L. J. Missaggia, R. J. Bailey, and A. Napoleone, "Strained-layer InGaAsP diode lasers with tapered gain region for operation $\lambda = 1.3$ μm," *IEEE Photon. Technol. Lett.*, vol. 6, pp. 1286–1288, Nov. 1994.

[65] E. S. Kintzer, J. N. Walpole, S. R. Chinn, C. A. Wang, and L. J. Missaggia, "High-power strained layer amplifiers and lasers with tapered gain regions," *IEEE Photon. Technol. Lett.*, vol. 5, pp. 605–608, 1993.

[66] H. Sato, M. Aoki, M. Takahashi, M. Komori, K. Uomi, and S. Tsuji, "1.3 μm beam-expander integrated laser grown by single-step MOVPE," *Electron. Lett.*, vol. 31, no. 15, pp. 1241–1242, 1995.

[67] K. Shinoda, K. Hiramoto, M. Sagawa, T. Toyonaka, and K. Uomi, "Circular beam, high power operation of 0.98 μm InGaAs/InGaAsP lasers with a tapered waveguide spot-size expander," *Electron. Lett.*, vol. 32, no. 12, pp. 1101–1102, 1996.

[68] R. Zengerle, B. Hübner, C. Gréus, H. Burkhard, H. Janning, and E. Kuphal, "Monolithic integration of spot-size transformer for highly efficient laser fiber coupling," *Electron. Lett.*, vol. 31, no. 14, pp. 1142–1143, 1995.

[69] M. Wada, M. Kohtoku, K. Kawano, H. Okamoto, Y. Kadota, Y. Kondo, K. Kishi, S. Kondo, Y. Sakai, I. Kotaka, Y. Noguchi, and Y. Itaya, "High-coupling-efficiency laser diodes integrated with spot-size converters fabricated on 2 inch InP substrates," *Electron. Lett.*, vol. 31, no. 24, pp. 2102–2103, 1995.

[70] A. Kasukawa, N. Iwai, N. Yamanaka, and N. Yokouchi, "Output beam characteristics of 1.3 μm GaInAsP/InP SL-QW lasers with narrow and circular output beam," *Electron. Lett.*, vol. 31, no. 7, pp. 559–560, 1995.

[71] I. F. Lealman, L. J. Rivers, M. J. Harlow, S. D. Perrin, and M. J. Robertson, "1.56 μm InGaAsP/InP tapered active layer multiquantum well laser with improved coupling to cleaved single mode fiber," *Electron. Lett.*, vol. 30, no. 11, pp. 857–859, 1994.

[72] I. F. Lealman, L. J. Rivers, M. J. Harlow, and S. D. Perrin, "InGaAsP/InP tapered active layer multiquantum well laser with 1.8 dB coupling loss to cleaved singlemode fiber," *Electron. Lett.*, vol. 30, no. 20, pp. 1685–1687, 1994.

[73] I. F. Lealman, B. M. Macdonald, J. V. Collins, P. J. Fiddyment, C. A. Jones, R. G. Waller, M. J. Robertson, L. J. Rivers, C. M. Peed, K. Cooper, S. D. Perrin, M. W. Niel, and M. J. Harlow, "Tapered active laserdevice performance and its impact on low cost optoelectronics," in *Proc. 8th Annu. Meet. IEEE Lasers and Electro-Optics Soc.*, 1995, pp. 11–12, paper MEMGW 2.2.

[74] R. Y. Fang, D. Bertoni, M. Meliga, I. Montrosset, G. Olivetti, and R. Paoletti, "Low-cost 1.55 μm InGaAsP-InP spot size converted (SSC) laser with conventional active layers," *IEEE Photon. Technol. Lett.*, vol. 9, pp. 1084–1086, Aug. 1997.

[75] Y. Tohmori, Y. Suzaki, H. Oohashi, Y. Sakai, Y. Kondo, H. Okamoto, Y. Kadota, O. Mitomi, Y. Itaya, and T. Sugie, "High temperature operation with low-loss coupling to fiber for narrow-beam 1.3 μm lasers with butt-jointed selective grown spot-size converters," *Electron. Lett.*, vol. 31, no. 21, pp. 1838–1839, 1995.

[76] M. Muramaki, "Mitsubishi Laser diode achieves 11° spread angle," *Semiconduct. Int.*, Dec. 1995, pp. 48.

[77] A. Kasukawa, N. Yamanaka, N. Iwai, Y. Nakahira, and N. Yokouchi, "Structural dependence of 1.3 μm narrow beam lasers fabricated by selective MOCVD," *Electron. Lett.*, vol. 32, no. 14, pp. 1304–1305, 1996.

[78] H. Soda, H. Kobayashi, T. Yamamoto, M. Ekawa, and S. Yamazaki, "Tapered thickness waveguide InGaAsP/InP BH MQW lasers," in *Proc. 8th Annu. Meet. IEEE Lasers and Electro-Optics Soc.*, 1995, p. 13, paper EMGW2.3.

[79] L. N. Langley, D. J. Robbins, P. J. Williams, T. J. Reid, I. Moerman, X. Zhang, P. Van Daele, and P. Demeester, "DFB laser with integrated waveguide taper grown by shadow masked MOVPE," *Electron. Lett.*, vol. 32, no. 8, pp. 738–739, 1996.

[80] G. Vermeire, F. Vermaerke, I. Moerman, J. Haes, R. Baets, P. Van Daele, and P. Demeester, "Monolithic integration of a SQW laser diode and a mode-size converter using shadow masked MOVPE growth," *J. Cryst. Growth*, vol. 145, pp. 875–880, 1994.

[81] K. Kawano, M. Kohtoku, H. Okamoto, Y. Itaya, and M. Naganuma, "Comparison of coupling characteristics for several spot size-converter-integrated laser diodes in the 1.3 μm wavelength region," *IEEE Photon. Technol. Lett.*, vol. 9, pp. 428–430, Apr. 1997.

Ingrid Moerman (M'96) was born in Gent, Belgium, in 1965. She received the degree in electrical engineering and the Ph.D. degree from the University of Gent, Gent, Belgium, in 1987 and 1992, respectively.

Since 1987, she has been with the Interuniversity Micro-Electronics Centre (IMEC) at the Department of Information Technology (INTEC) of the University of Gent. Her main contributions are the epitaxial growth of InGaAsP-InP and In(Al)GaAs–GaAs laser diodes and waveguiding devices. In 1997, she became a permanent member of the Research Staff at IMEC, where she coordinates the research on the epitaxial growth of III–V optoelectronic devices.

Peter P. Van Daele (M'91) was born in 1961. He received the Ph.D. degree in electrical engineering in 1988 from the University of Gent, Gent, Belgium.

He became a permanent Member of Staff from the Interuniversity Micro-Electronics Centre (IMEC) at the Department of Information Technology (INTEC) of the University of Gent, where he is responsible for the research on processing and packaging of III–V optoelectronics devices. In 1993, he also became part-time Professor. He is author and coauthor of about 200 publications in the field of optoelectronic components and technology.

Piet M. Demeester (M'89) received the degree in electrical engineering and the Ph.D. degree from the University of Gent, Gent, Belgium, in 1984 and 1988, respectively.

Since 1987, he has been employed by the Interuniversity Micro-Electronics Centre (IMEC) and works in the Department of Information Technology at the University of Gent, where he is a part time Professor. He is coordinating the research on the epitaxial growth of III–V optoelectronic devices and on the design and modeling of broad-band communication networks.